

We are IntechOpen, the world's leading publisher of Open Access books Built by scientists, for scientists

6,900

Open access books available

186,000

International authors and editors

200M

Downloads

Our authors are among the

154

Countries delivered to

TOP 1%

most cited scientists

12.2%

Contributors from top 500 universities



WEB OF SCIENCE™

Selection of our books indexed in the Book Citation Index
in Web of Science™ Core Collection (BKCI)

Interested in publishing with us?
Contact book.department@intechopen.com

Numbers displayed above are based on latest data collected.
For more information visit www.intechopen.com



Biomass Estimation Using Satellite-Based Data

Patrícia Lourenço

Abstract

Comprehensive measurements of global forest aboveground biomass (AGB) are crucial information to promote the sustainable management of forests to mitigate climate change and preserve the multiple ecosystem services provided by forests. Optical and radar sensors are available at different spatial, spectral, and temporal scales. The integration of multi-sources sensor data with field measurements, using appropriated algorithms to identify the relationship between remote sensing predictors and reference measurements, is important to improve forest AGB estimation. This chapter aims to present different types of predicted variables derived from multi-sources sensors, such as original spectral bands, transformed images, vegetation indices, textural features, and different regression algorithms used (parametric and non-parametric) that contribute to a more robust, practical, and cost-effective approach for forest AGB estimation at different levels.

Keywords: aboveground biomass, regression algorithms, machine learning algorithms, remote sensing, satellite-derived predictor variables

1. Introduction

The aboveground biomass (AGB) of forests directly provides the amount of organic matter in living and dead plant materials, for example, of leaves, branches, and stem, and it is expressed in dry weight per unit area [1]. AGB is also one of the major reservoirs of carbon in forest ecosystems and a key indicator of forest health [2]. Thus, measuring and monitoring AGB changes is crucial to understanding AGB role in the global carbon cycle to reduce carbon dioxide concentrations and to mitigate climate change [3]. AGB was recognized as an Essential Climate Variable by the United Nations Framework Convention on Climate Change (UNFCCC) [4] and an essential biophysical parameter of forest ecosystems [5] for estimating carbon and water cycling, and energy fluxes between land surface and atmosphere. These are processes relevant on the background of climate change [6]. In addition, AGB resources underlie the development of a bio-based economy as part of the European Union Forest-Based Vision targets sector 2030 [7]. The key role of AGB forests leads to the need for accurate and precise estimates of AGB to assess changes in forest structure, including understanding the roles of forests in the terrestrial carbon flux and global climate change [8].

Spatial and temporal quantification and monitoring of AGB are important to assess the impacts of climate and land use changes on the global carbon cycle and understand the causing effects on ecosystem resilience [5]. Fast, accurate and

timely estimation and monitoring of AGB, at local, regional, and global scales, will significantly reduce the uncertainty in carbon stock assessments and provide valuable information to better support sustainable forest management strategies [9, 10]. The frequently used methods to estimate AGB are the indirect, which are based on mathematical relations between biomass, dependent variable and one or a few easy-to-measure tree variables, independent variables [11]. Traditionally, indirect methods use forest inventories and allometric functions at tree level to evaluate biomass at plot level and an extrapolation method to assess all area [12].

In last decade, there has been an increase of biomass mapping and estimations for global terrestrial ecosystems using remote sensing (RS) [6]. Satellite-derived predictor variables have been used to estimate AGB and assess its spatio-temporal variability through valuable RS approaches [13]. The development and implementation of RS-based AGB estimation' monitoring frameworks may provide low-cost and accurate operational geospatial tools for rapidly and effectively detecting, mapping and assessing relevant changes in AGB in any study area. On the other hand, this same type of geospatial tool might be able to support the execution, monitoring, and impact evaluation of nature conservation policies and strategies, by providing a systematic and accurate forest AGB estimation monitoring system [14]. RS provides variables indirectly related to AGB, and the spectral response (original or transformed sensor bands) of the vegetation cover, density, shade, and texture is correlated with AGB [15].

In response to the urgent need for much improved mapping of global forest biomass and the lack of current space systems capable of meeting this need, the BIOMASS mission arose from European Space Agency (ESA) as an Earth observing satellite planned to launch in October 2022 [16]. BIOMASS mission aims to provide the scientific community with accurate maps of world's forest biomass, including height, state, disturbance patterns, and how they are changing [17, 18]. Gathering BIOMASS mission information with the economic and environmental knowledge will enable to reach a better spatial planning of the forest AGB [19].

The objective of this chapter is to present the satellite images, satellite-derived predictor variables and algorithms used to estimate forest AGB with RS data. To accomplish this objective, the Section 2 presents the types of satellite sensors used in RS. The Section 3 describes the satellite-derived predictor variables. In Section 4, there is a description of the most used algorithms to predict forest AGB. Section 5 presents a discussion of the more frequently used satellite images, algorithms, and variable importance for AGB estimation with RS. Finally, in Section 6, the main conclusions are presented.

2. Remote sensing satellite sensors

Currently, there is a wide variety of RS data available for forest AGB estimation, such as optical (passive) and radar (active) sensors data, at different spatial, spectral, and temporal scales resolution, from local to global scale, with or without costs [20]. The selection of the proper satellite data it will depend on the scope of the research and on the study area, considering the area size, type of forest, and available budget to obtain accurate forest AGB estimations. Optical and radar RS follow similar approaches for forest AGB analysis, modeling, mapping, and monitoring [21]. Optical RS imagery gives spectral information of the horizontal forest structure [22], while radar RS imagery gives information of the vertical forest structure due to the ability of penetrating the forest canopy to a certain depth [23].

The analyze of optical data is easier to use than radar RS data because, after calibrating and correcting the images, the data can be directly processed and

extracted and similarly interpreted as a photograph. As passive sensor, optical RS sensors need a light source (e.g., sun light), and the quality of the images is dependent of the weather and day light. These sensors record a variety of electromagnetic spectrum radiation frequency, especially at wavelengths of visible light and infra-red. Optical RS sensors record the reflectance of the electromagnetic spectrum of earth objects in the visible (Blue, Green, and Red) and infrared regions (near infrared – NIR and short wave infrared – SWIR). Visible and NIR (VNIR), and SWIR are the wavelengths more sensitive to vegetation characteristics.

Optical RS data are widely used to estimate AGB of different types of forest, such as in temperate forests [24], Mediterranean forests [25], sub-tropical forests [26], and boreal forests [27]. Different types of spatial resolution sensors (low: 100–1000 m, and medium: 10–100 m) have been used in studies of AGB estimation at global, regional, and local scale, such as MODIS [15], Landsat ETM+ [28], SPOT [29], and more recently Sentinel-2 [30]. Very high spatial resolution sensors (<1 m), such as IKONOS, Quickbird II, WorldView-2, have advantage over low and medium spatial resolution sensors, despite their cost. These sensors provide finer spatial scale with a greater thematic resolution and accuracy which can be used to complement AGB forestry measurements from the forest inventory [31, 32]. Monitoring and evaluation of AGB estimation over time can be performed by using optical RS due to existing continuous data and wide spatial coverage. However, despite the widespread usage of optical RS data in the estimation of forest AGB, these are limited to their poor penetration capacity in the forest canopies and clouds, in addition to presenting problems of data saturation in high AGB density [33].

On the contrary, interpretation of radar RS sensor data, that is, Synthetic Aperture Radar (SAR) and Light Detection and Ranging (LiDAR) sensors imagery, is not always straightforward because of the signal being responsive to surface characteristics, like structure and moisture, and consequently to have the non-intuitive and side-looking geometry. Despite that, radar provides much more information than just an image to be visually analyzed because of being characterized by two data values for each pixel, a Magnitude value (image analogous to one collected by an optical sensor) and a Phase value (it cannot be visually interpreted). As an active sensor, radar has the advantage of providing its light source and enabling it to operate 24 hours a day.

SAR sensors have been used to estimate forest AGB to complement the spectral reflectance characteristics of vegetation in the optical regions and are very useful in regions often covered by clouds [34]. These sensors are sensitive to water content in vegetation and register information independently of the weather conditions [35] through the interaction of the radar waves with tree scattering elements [17]. The techniques most used in biomass studies using SAR data are regression based on backscattering amplitudes [36] and interferometry based on backscattering amplitudes and phases [37]. The important factors in the backscattering coefficient are wavelength (e.g., K, X, C, L, P), polarization (e.g., HH, VV, HV, VH), incidence angle, land cover, and terrain properties (e.g., roughness and dielectric constant).

The short wavelength X and C bands, which interact only with tree canopy surface layer information, are more suitable for AGB estimation in areas with low biomass [38]. The long wavelength L and P bands are more suitable for AGB estimation of dense forest with relatively high biomass density for presenting greater interaction with the forest elements, such as branch, stem, and soil under the canopy [39] and by allowing canopy height to be retrieved by polarimetric interferometry [17].

The polarization information can be linear and crossed. The linear polarization is obtained through linear transmission and reception signal, horizontal (H) and

vertical (V), HH and VV, respectively [40]. In the cross-polarization, the transmission and reception signal are different, i.e., HV and VH. Cross-polarized VH backscatter has been considered the largest dynamic range and the highest correlation with biomass [17]. In the case of linear polarization, ground conditions can affect the biomass-backscatter relationship. HH backscatter comes mainly from stem-ground scattering, while VV backscatter results from both volume and ground scattering.

SAR sensors have been used in several forest AGB estimation studies, such as in Miombo Savanna Woodlands [41], deciduous broadleaved and mixed broadleaf-conifer forests [30, 42], tropical peat swamp forests [43], tropical savannas and woodlands [44], temperate deciduous forest [45], rainforest [46], coniferous temperate forest [47], and mixed and deciduous boreal forest [48]. Currently, there is a considerable number of ongoing SAR missions from various agencies, namely Sentinel-1A,B, ALOS-2, SOCOM-1a,b, Cosmo-SkyMed SG, and PAZ. For historical analysis, it can use data from sensors, such as, ERS-1,2, JERS, Envisat, Radarsat-1,2, ALOS, TerraSAR-X, and TanDEM-X. However, despite the positive correlation with the forest structure parameters, SAR data can present saturation problems. The saturation problems can be over different types of temperate, boreal, and tropical forests [49] and depend on the wavelengths, L band at around 100–150 t/ha [50] and 250 t/ha [51], polarization, characteristics of the vegetation stand structure and ground conditions [52]. Furthermore, estimating AGB with only SAR data is difficult, since these data provide information on the roughness of the land cover surfaces and do not distinguish the types of vegetation [53].

LiDAR is an active RS method sensor composed by a laser, a scanner and a specialized GPS receiver used from spacecraft satellite for Space-borne Laser Scanning (SLS), aircraft for Airborne Laser Scanning (ALS) – the most used in forestry approaches – and on the ground level, Terrestrial Laser Scanning (TLS). LiDAR uses pulsed laser light to measure ranges (variable distances) to the object Earth. Differences in return times and laser wavelengths serve to calculate distance traveled which is then converted to elevation. These measurements generate a cloud of points that allow the 3D representation of the vegetation, based on the identification of the X, Y, and Z location, and can penetrate within forest canopy [54]. The airborne LiDAR has the advantage of covering a large area, allowing its use in large areas with minimum occlusion of the terrain by vegetation. Also, it does not saturate even at very high biomass levels (>1000 Mg/ha) [55].

LiDAR provides accurate measurements of vegetation structures, such as height, crown size, basal area, stem volume, and vertical profile. These measurements to characterize the canopy or crown cover in three dimensions and consequently to estimate forest AGB in any study area [56]. The LiDAR metrics can be extracted on the basis of either individual trees [57] or areas [49]. The extraction of these metrics depends on the laser return signal (discrete-return vs. waveform), scanning pattern (scanning or profiling), and footprint size (small vs. large). LiDAR data have been used to estimate forest AGB in combination with other sensors data (optical and/or radar) [15, 58]. Moreover, LiDAR data are a good complement to forest inventory data because they capture spatial variability and can be acquired quickly and in large or difficult to access areas [58]. However, the limited availability and the cost of these data prevent its extensive application [10].

Integration of multi-source RS data, that is, optical, SAR or/and LiDAR data, is important to improve AGB estimation because more information about forest structure features is integrated than just by a sensor. The integration of multiple data sources for more accurate forest AGB estimations has been explored by several authors [44, 59, 60]. In this way, the advantages of each sensor are highlighted to the detriment of negative characteristics of the sensors [61]. Nevertheless, RS data

should be complemented with AGB field data measurements, as training and validation data, in order to improve the accuracy of the AGB estimation model [6].

3. Satellite-derived predictor variables

In studies of forest AGB estimation, it is important to integrate different types of independent variables derived from passive and active sensors, such as original spectral bands, transformed images, vegetation indices, and textural variables (**Table 1**), to achieve accurate predictive models [62].

Spectral bands (e.g., VNIR and SWIR) reflect the vegetation structure, texture, and shadow, related with leaf cellular structure and plant pigments, which are correlated with AGB [15]. VNIR wavelengths are more sensitive to pigments and overall canopy health, while SWIR capture many biochemical, leaf mass per area, and discriminates moisture content of soil and vegetation [15]. In Red region occurs absorption by chlorophyll, while in NIR region, there is a pronounced reflection by mesophyll cells [69]. Green band is related with the greenness of vegetation representing the absorption intensity of Blue and Red energy by plant leaves and the reflection intensity of green energy [70]. On the other hand, hyperspectral sensors allow to have many narrow contiguous spectral bands and can accurately discriminate absorption features' wavelength position and shape.

Transformed images have been used to reduce the dimension of the data, required for optimal performance, by producing new variables from optical multispectral data [21]. There are some image transformation techniques, such as Principal Component Analysis (PCA), Minimum Noise Fraction transform (MNF), and Tasseled Cap Transform (TCT). PCA is the most used transformed image to enhance the change information from stacked multisensor data and captures maximum variance generating a new reduced set of bands in which the information is concentrated and that have little correlation [71]. For n bands of multispectral data, the first PC (PC1) includes the largest percentage of the total image variance and the succeeding components (PC2, PC3, ..., PC n) each containing a decreasing percentage of the scene variance [70].

MNF transform is a linear transformation of the reflectance data of hyperspectral and high spectral resolution images to determine the inherent dimensionality of image data, to segregate noise in the data, and to reduce the computational requirements for subsequent processing [72, 73]. MNF is composed of two PCA rotations that separate the noise from the data. The first rotation consists in the call noise whitening process in which the principal components of the noise covariance matrix are used to decorrelate and rescale the noise in the data

Sensor	Variable	Description	References
Optical	Spectral features	Spectral bands, vegetation indices, and transformed images	(e.g. [62])
	Spatial features	Textural images	(e.g. [63])
Active	Radar	Backscattering coefficients, textural images, interferometry SAR, and Polarimetric SAR interferometry	(e.g. [38, 64–66])
	LiDAR	Lidar metrics based on statistical measures of point clouds or estimated products (e.g. canopy height or individual trees)	(e.g. [67, 68])

Table 1.
Optical and active sensor derived variables used in forest AGB estimation.

and obtain transformed data. The transformed noise data have unit variance and no band-to-band correlations. The second rotation uses the principal components derived from the noise whitening process and rescaled by the noise standard deviation. The inherent dimensionality of the second transformation data is determined by examining the final eigenvalues and the associated images. In this way, MNF transformation may reduce the dimensionality of hyperspectral image data, eliminate correlations band-to-band, and order components in terms of image quality [74].

TCT is a conversion of the original bands of an image into a new set of bands through an orthogonal transformation with defined interpretations, useful for vegetation mapping, and directly associated with important physical parameters of the vegetation [75]. TCT uses a similar concept to the PCA in which linear combinations of the original image bands are performed. The tasseled-cap band are produced as the sum of image band 1 times a constant plus image band 2 times a constant, etc. The coefficients used to create the tasseled-cap bands are derived statistically from images and empirical observations and are specific to each imaging sensor. TCT aims to compress the spectral data in few bands associated with physical scene characteristics with minimal information loss [76]. These bands are then correlated, transforming them orthogonally into a new set of axes associated with physical features. The resulting spectral features consists in three axes defined as brightness, greenness, and wetness that are directly associated with important physical parameters [77]. Brightness – the first feature of TCT – is a weighted sum of all the bands and is related with bare or partially covered soil, natural and man-made features, and variations in topography [70]. Greenness – the second feature of TCT – is a measure of the contrast between the NIR band and the visible bands and is related with vegetation amount in the image. Wetness – the third feature of TCT – is orthogonal to the first two components and is related to canopy and soil moisture [78]. TCT was developed in 1972 for the Landsat multi-spectral scanner (MSS) to understand the growth patterns of plants, soil moisture, and other hydrological features in the spectral space formed by combinations of different bands but is adapted to current sensors.

Vegetation index is a spectral transformation of at least two bands to improve the contribution of the vegetation properties of an image. The wide variety of vegetation indices are calculated based on the ratio between two or more bands to contrast the high absorption by leaf pigments (chlorophylls, carotenoids, and xanthophylls) in the visible spectral region (400–700 nm), high reflectance by leaves in the NIR region (700–1300 nm), and moderate water absorption in the SWIR (1300–2100 nm) [79]. There is a wide range of vegetation indices that are used in the estimation of AGB (**Table 2**).

Two most common vegetation indices used in forest AGB estimation are NDVI and SR [63]. NDVI is the fraction of the difference and the sum of the NIR and Red bands where chlorophyll absorbs Red whereas the mesophyll leaf structure scatters NIR [80]. SR is the ratio between NIR and RED [81] and intends to capture the contrast between the RED and NIR bands for vegetated pixels. Both vegetation indices prove to have a good relation with the AGB estimation derived from satellite images data in several types of forests [63, 82]. Further, canopy moisture content can be quantified through vegetation water indices, namely NDWI which is related with NIR and SWIR bands [83].

Texture is a feature used to identify objects or regions of interest in an image [105], based on mathematical pattern (spatial) analysis. Texture is characterized by defining local spatial organization of spatially varying spectral values that is repeated in a region of larger spatial scale. The variations in these scales in the image values that constitute texture are generally due to an underlying physical variation

Vegetation indices		Formulation	Reference
Normalized difference vegetation index	NDVI	$\frac{NIR-RED}{NIR+RED}$	[84]
Enhanced vegetation index	EVI	$G \times \frac{NIR-RED}{NIR-C1 \times RED-C2 \times BLUE+L}$ Note: C1 = 6; C2 = 7.5; L = 1; G = 2.5	[85]
Modified simple ratio	MSR	$\frac{\frac{NIR}{RED}-1}{\sqrt{\frac{NIR}{RED}+1}}$	[86]
Specific leaf area vegetation index	SLAVI	$\frac{NIR}{RED+SWIR}$	[87]
Soil-adjusted vegetation index	SAVI	$(1+L) \times \frac{(NIR-RED)}{NIR+RED}$	[88]
Triangular vegetation index	TVI	$\sqrt{\frac{NIR-R}{NIR+RED}} + 0.5$	[89]
Corrected transformed vegetation index	CTVI	$\frac{NDVI+0.5}{ABS(NDVI+0.5)} \times \sqrt{ABS(NDVI+0.5)}$	[90]
Transformed triangular vegetation index	TTVI	$\sqrt{ABS\left(\frac{NIR-RED}{NIR+RED} + 0.5\right)}$	[91]
Ratio vegetation index	RVI	$\frac{RED}{NIR}$	[92]
Normalized ratio vegetation indexes	NRVI	$\frac{RVI-1}{RVI+1}$	[93]
Infrared percentage vegetation index	IPVI	$\frac{NIR}{NIR+RED}$	[94]
Optimized soil-adjusted vegetation index	OSAVI	$\frac{NIR-RED}{NIR+RED+Y}$ Y = 0.16	[95]
Normalized difference index using bands 4 & 5 of Sentinel-2	NDI45	$\frac{RE1-RED}{RE1+RED}$	[96]
Inverted red-edge chlorophyll index (Sentinel-2)	IRECI	$\frac{RE3-RED}{RE1/RE2}$	[97]
Transformed normalized difference vegetation index	TNDVI	$\sqrt{\frac{NIR-RED}{NIR+RED}} + 0.5$	[98]
Sentinel-2 red-edge position	S2REP	$705 + 35 \times \frac{\left(\frac{NIR+RED}{2}\right) - RE1}{RE2-RE1}$	[97]
Green normalized difference vegetation index	GNDVI	$\frac{NIR-GREEN}{NIR+GREEN}$	[99]
Simple ratio	SR	$\frac{NIR}{RED}$	[100]
Green ratio vegetation index	GRVI	$\frac{GREEN-RED}{GREEN+RED}$	[101, 102]
Normalized difference water index	NDWI	$\frac{NIR-SWIR}{NIR+SWIR}$	[83, 103]
Moisture stress index	MSI	$\frac{NIR}{SWIR}$	[104]

Table 2.
Vegetation indices used to establish the AGB model.

in the landscape that changes reflectivity or emissivity [106]. Textural analysis techniques can be used to provide quantitative metrics that are highly sensitive to the underlying processes of change [107]. However, as the texture has many different dimensions, there is no single texture representation method that is suitable for a variety of textures. There are several methods of extracting textures from RS images; however, texture measurements based on the gray level co-occurrence matrix (GLCM) [105] is one of the most used in forest AGB estimation [64, 108]. The extraction of appropriate descriptions of texture involves selecting moving window sizes which in GLCM is a key parameter in texture analysis [106, 109]. Theoretically, variation and contrast should increase with increasing size and displacement of the window until the size of the textured objects is reached [108].

Overall, small windows produce noisier estimates of the texture descriptor and maintain a high spatial resolution, while larger windows amplify the estimation errors near spatial instances. Due to the variety of objects in an image, when estimating texture parameters should not be used a fixed window. The estimation of texture parameters should be done based on the directional invariant measures, which are the averages between the texture measures of four directions (0, 45, 90,° and 135°) [110]. There are also 8 statistical texture measures, from 14 suggested by Haralick [105], considered the most relevant for the analysis of RS images: angular second moment, contrast, variance, homogeneity, correlation, entropy, mean, and dissimilarity [64]. The information of each of these texture measures depends on the type of image to be analyzed in relation to the spectral domain, the spatial resolution and characteristics of detected objects (size, shape, and spatial distribution). In addition, when faced with a complex forest structure textural images have stronger relationships with biomass than the original spectral bands [64].

4. Algorithms to predict forest AGB

Forest AGB estimated from RS data is usually via an indirect relationship between the spectral response (original or transformed sensor bands) and AGB calculations based on field measurements, allowing an extrapolation of field data collected for larger scales [111, 112]. Different prediction methods can be applied to estimate forest AGB [52, 113]. The most used methods for forest AGB estimation are the linear and multiple regression models [114]. However, in recent years' machine learning methods, such as, random forest (RF), support vector machines (SVM) and artificial neural network (ANN) have become more prevalent [113].

Linear and multiple regression models are parametric algorithms which assumes that there is a linear relationship between both the dependent (i.e., AGB) and independent (derived from DR) variables [115]. Simple linear regression establishes a relationship between a dependent and one independent variable. If there is a relationship between two or more independent variables, the regression is called multiple linear regressions. Multiple regressions can be linear and nonlinear. This type of regression also allows to determine the relative contribution of each of the independent variables to the total explained variance and the explained variation of the model. Despite being an easy method to calculate the relationship between RS-derived variables and forest AGB, parametric algorithm is not simple global linear because it is affected by many factors (e.g., forest age, tree species, and tree height). Thus, a stepwise regression model might be applied to identify the appropriate RS-derived variables that present strong relations with forest AGB [114].

Among the existing non-parametric algorithms, only the most commonly applied to predict forest AGB estimation using RS data will be described, that is, RF, SVM and ANN [10, 52]. Non-parametric algorithms are more flexible than the parametric algorithms and create more complex models of non-linear AGB. These machine learning methods are a more reliable technique to estimate AGB [8] because do not have predefined model structures and the data determined the structure of the model.

RF is a machine learning classification and regression technique that creates a vast number of uncorrelated decision trees at training time, where the most accurate decision tree can be voted [116]. In addition, regression tree-based methods have a higher potential to identify non-linear relationships between dependent and independent variables [117]. This advantage is significant for RS-based studies, where data have shown low linear relation with AGB and the variables might be collinear [113]. RF has also the advantage of using multisource data in large study areas [10].

SVM is a machine learning algorithm that analyzes data used for classification and regression analysis [118]. This algorithm, from a set of category-identified training examples, build a model in which the new examples are attribute to one category or another. SVM constructs a linear separation rule between examples in a higher-dimensional space induced by a mapping function in training samples. This algorithm has the ability to use small data training samples to produce relatively high estimates of forest biophysical parameters using remote sensing data [10].

ANN is an important non-parametric model for forest parameter estimation [119] that simulates the associative memory as animal brain [120]. This algorithm learns by processing examples that have one or more inputs (independent variables from different data sources, such as RS and ancillary data) and known results, establishing associations by probability that will contribute to the “learning.” These associations are stored in their net data structure. After receiving several examples, the net is able to predict the results from inputs using the previously established associations. Thus, the greater the number of examples, the greater the accuracy of ANN’s predictions will be. However, the relationship between the dependent and the independent variable is not easily interpreted [10].

Accurate predictive models of forest AGB are of great importance for forest management and climate mitigation [121]. In general, there are three widely used methods of validation of forest AGB estimation. According to Lu et al. [10], the first method consists in selecting a set of sample plots through random, systematic, and stratified random sampling. The sample plots will be randomly divided into two subsets. One of the subsets will be used to train the model (e.g., 75% of subset data), while the other will be used to calibrate the model (e.g., 25% of subset data). In this case, both subsets are produced from the same sample plot which may lead to an overestimation of accuracy. The second method is cross-validation where a set of sample plots is selected using one of the first sampling previous methods. Here, a plot sample is removed while the remaining plots are used for the development of forest AGB estimation model. This method has a similar advantage to the first; however, it presents a more reliable precision assessment. The third method involves the use of an independent set of sample plots collected through a sampling design. However, despite being theoretically reliable, this method is more expensive.

These accuracy statistics are often expressed as the coefficient of determination (R^2), a measure of how well model predictions explain the target variance of the validation set, and the root mean square error (RMSE), a frequently used measure that indicates the absolute fit of the model to the data (i.e., how close the observed data points are to the model’s predicted values). RMSE is a good measure of how accurately the model predicts the response, and it is the most important criterion for fit if the main purpose of the model is a prediction [122]. In general, a high R^2 and a low RMSE value shows a good adjustment between the model developed and the sample plot data. Thus, obtaining an accurate predictive model of forest AGB estimation is important to provide valuable information to better support sustainable forest management strategies to mitigate climate change and preserve the multiple ecosystem services provided by forests.

5. Discussion of forest AGB estimation using RS data

Over the past decades, there has been an improvement in satellite data from sparse coarse to medium and fine spatial resolutions, allowing better accuracy in estimating forest AGB at local, national, and global scale [69]. Recently with the launch of the Sentinel satellite family, more accurate predictive models of forest AGB estimation may be produced due to the existence of better spatial (bands with

10, 20, and 60 m) and spectral resolutions data, with a 5 days' revisit time of these satellite family in comparison with other free commercial satellite data, as Landsat or MODIS [59]. For instance, Landsat images with spatial resolution of 30 m contain many mixed pixels, and a pixel can contain different trees species and vegetation ages. In addition, large amount and good quality of field measurements, obtained from forest inventory plots data [123, 124] and/or from LiDAR data [125] should be used, as training and calibration data, to obtain accurate model of forest AGB estimation.

More recently, the studies of forest AGB estimation have been using the combination of optical and radar data. The integration of different remotely detected data sources showed to increase the accuracy of the predictive models of forest AGB estimation. In this way, the incorporation of forest structural parameters of SAR data overcome the problems of mixed pixels and data saturation caused by optical data [30, 126]. For instance, Townsend [127] observed that the model's performance for estimating biophysical properties of forests has improved due to the capabilities of the Landsat TM and SAR data. On the other hand, Forkuor et al. [44] when mapping forest AGB found better predictive accuracy of AGB when combining optical and SAR sensors (Sentinel-1 and 2) than individually. However, several authors corroborate that optical sensors produce better forest AGB estimation results than SAR when used individually [8, 44, 128] despite the lack of sensitivity of the optical data to AGB beyond the canopy closure and grass interference in savannas and forests [129, 130].

In the last years, predictive models to estimate forest AGB have been applying machine learning algorithms based on decision trees instead of the traditional parametric regression models [59]. Machine learning algorithm (e.g., ANN) showed advantage over regression algorithms for being versatile and flexible [131]. This advantage was observed by Ou et al. [132] when comparing with two parametric models (linear regression model and linear regression with combined variables), the two non-parametric models (RF and ANN) resulted in significantly greater estimation accuracies of forest AGB, that is, higher coefficient of determination (R^2) and lower root mean square error (RMSE). Other authors corroborate with this statement by showing that non-parametric models have greater capacity to better capture the heterogeneity of forest AGB compared to parametric models [47, 64, 128, 133].

Among the variety of machine learning techniques, RF algorithm revealed to be one of the best methods for classification and regression by providing high accuracy in estimating forest AGB, high speed of computation, robustness and capacity to predict the important variables either using optical or SAR data [30, 59, 128, 134–137]. Also, RF showed to be suitable for analyzing a larger data set, while other non-parametric algorithms, such as support vector regression (SVR), are more suitable to be used with small data set [30, 47] and in grasslands and shrubs AGB estimations [138]. However, regardless of the algorithm applied to the model (e.g., linear regression, RF, and ANN), independent variables seem to be more important to obtain accurate forest AGB estimations [30].

The predictive models are able to explore and rank the variables importance measure in the forest AGB estimation. Textural features from optical data (spectral data) and SAR (backscattering data), spectral vegetation indices, and, more recently, biophysical variables derived from Sentinel-2 (e.g., LAI - Leaf area index, FVC - Fractional vegetation cover, and FAPAR - fraction of photosynthetically active radiation) have been considered as the most important variables for forest AGB estimation [30, 47, 141–145]. Spectral bands produce predictive models with lower accuracy than using vegetation indices, transformed images and textural features [132]. Therefore, Forkuor et al. [44] showed that SWIR bands are

important in predictive models of AGB estimation in semi-arid regions. In addition, the integration of variables (e.g., multispectral bands, transformed images, vegetation indices, and textural features) from optical and SAR sensors provide more accurate predictive models of forest AGB estimation [10, 52] than simple backscatter (SAR) and spectral (optical) bands [30, 47, 141, 142].

Vegetation indices are still important variables to estimate forest AGB as reported by several authors [59, 107, 134, 139, 140]. In last years, due to the Multi-Spectral Instrument aboard of the Sentinel-2 satellite, two relatively new vegetation indices, NDI45 and IRECI emerged (**Table 2**). Both new vegetation indices take advantage of the Sentinel-2 Red-edge bands (band 5 = 705 nm; band 6 = 740 nm; band 7 = 783 nm) to reduce the effects of saturation problem in high AGB density [44]. NDI45 is similar to NDVI but the original NIR band of 800 nm [84], is replaced by the new Red-edge band (band 5) and the Red band (band 4 of 665 nm) is kept [96]. On the other hand, IRECI uses the three available Red-edge bands of Sentinel-2 and put little emphasis in the red band to avoid saturation problem [97].

Transformed images, such as PCA, are also an important variable to face the saturation problem of optical sensor at low to intermediate biomass levels (between 60 and 150 Mg/ha) [146]. These images can also be used as input for textural images of optical and SAR sensors to prevent the saturation problem of high AGB density. For instance, textural variables showed to be more suitable to predict forest AGB estimation due to its ability to simplify complex cover structures, such as uneven-aged forests and different canopy structure than spectral bands [147, 148]. Also, textural bands from optical sensor images (e.g., sentinel-2, SPOT-6, and AVNIR) contributed to obtain accurate predictive models of forest AGB estimation than the original spectral bands [47, 132, 147, 149].

In addition, the greater interaction capacity of SAR-derived variables with the forest elements, such as branch, stem, and soil under the canopy [39, 65, 150], highlight their advantage over biophysical parameters (e.g., LAI, FVC, and FAPAR) to estimate forest AGB [44]. Hence, the importance of SAR long wavelengths (P-band), capable of providing accurate forest AGB estimations, will be harnessed in the BIOMASS mission to provide unprecedented information on the distribution of world's forest AGB and its changes [17, 18]. This mission will help to build a sustainable global system of monitoring and quantification of biomass over time to help countries in managing forest resources and mitigating the impacts of climate change and land use changes.

6. Conclusions

From the analysis of several forestry AGB estimation studies, the integration of optical and radar data improves the information extraction process, taking advantage of the strengths of different image data. In this way, mixed pixel problems and data saturation is reduced. Further, Sentinel satellite family showed to be promising free satellites data to reach accurate forest AGB estimation models, including in regions with few or scarce AGB information.

Non-parametric models, such as RF, SVM, and ANN, have been replacing regression models due to their greatest ability to capture the heterogeneity of forest AGB than parametric models. Among the variety of machine learning techniques, RF algorithm showed to be one of the most used with ability to obtain better accuracy in forest AGB estimation, either using optical or SAR data.

The integration of different data sources RS-derived, that is, spectral bands, transformed images, vegetation indices, textural features, showed good correlation with forest AGB. VNIR bands are the most important to calculate most of

vegetation indices. When using Sentinel-2 data, the available red-edge bands showed to reduce the effects of saturation problem in high AGB density.

PCA is a key variable to face the saturation problem of optical sensor of high AGB density and to be used as input data for textural features of optical and SAR sensors also to prevent the saturation problem of both sensors. Textural features, from both optical and SAR sensors, are among of the most suitable variables for forest AGB estimation due to their stronger relationships with AGB. SAR long wavelengths bands (L and P) showed to be very promising bands in studies of relatively high biomass density.

Acknowledgements

This work is funded by the National Funds through FCT - Foundation for Science and Technology under the Project UIDB/05183/2020 and by Programa Operativo de Cooperação Transfronteiriço Espanha-Portugal (POCTEP), and Programa INTERREG V A Espanha – Project IDERCEXA – Investigación, Desarrollo y Energías Renovables para nuevos modelos empresariales en Centro, Extremadura y Alentejo, 0330_IDERCEXA_4_E.

Author details

Patrícia Lourenço^{1,2,3}


1 MED - Mediterranean Institute for Agriculture, Environment and Development and Departamento de Engenharia Rural, Escola Ciências e Tecnologia, Universidade de Évora, Pólo da Mitra, Évora, Portugal

2 Research Center on Geo-Spatial Science, Faculty of Science of the University of Porto (CICGE), Vila Nova de Gaia, Portugal

3 Andalusian Center for the Evaluation and Monitoring of Global Change, University of Almeria (CAESCG), Almería, Spain

*Address all correspondence to: pmrlourencov2@gmail.com

IntechOpen

© 2020 The Author(s). Licensee IntechOpen. Distributed under the terms of the Creative Commons Attribution - NonCommercial 4.0 License (<https://creativecommons.org/licenses/by-nc/4.0/>), which permits use, distribution and reproduction for non-commercial purposes, provided the original is properly cited. 

References

- [1] Brown S. Estimating Biomass and Biomass Change of Tropical Forests: A Primer. Rome: Food & Agriculture Org; 1997
- [2] Brown S, Schroeder P, Birdsey R. Aboveground biomass distribution of US eastern hardwood forests and the use of large trees as an indicator of forest development. *Forest Ecology and Management*. 1997;**96**:37-47
- [3] Qureshi A, Badola R, Hussain SA. A review of protocols used for assessment of carbon stock in forested landscapes. *Environmental Science & Policy*. 2012; **16**:81-89
- [4] Sessa R, Dolman H. Terrestrial Essential Climate Variables for Climate Change Assessment, Mitigation and Adaptation. Rome: FAO GTOS; 2008. p. 52
- [5] Wang X, Shao G, Chen H, et al. An application of remote sensing data in mapping landscape-level forest biomass for monitoring the effectiveness of forest policies in northeastern China. *Environmental Management*. 2013;**52**: 612-620
- [6] Kumar L, Mutanga O. Remote sensing of above-ground biomass. *Remote Sensing*. 2017;**9**:935
- [7] FTP. Horizons - Vision 2030 for the European Forest-Based Sector. Forest-Based Sector Technology Platform. Brussels. 2013. pp. 1-10. Available from: www.forestplatform.org
- [8] Vafaei S, Soosani J, Adeli K, et al. Improving accuracy estimation of Forest aboveground biomass based on incorporation of ALOS-2 PALSAR-2 and sentinel-2A imagery and machine learning: A case study of the Hyrcanian forest area (Iran). *Remote Sensing*. 2018;**10**:172
- [9] Pan Y, Birdsey RA, Fang J, et al. A large and persistent carbon sink in the world's forests. *Science*. 2011;**333**:988-993
- [10] Lu D, Chen Q, Wang G, et al. A survey of remote sensing-based aboveground biomass estimation methods in forest ecosystems. *International Journal of Digital Earth*. 2016;**9**:63-105
- [11] Sousa AM, Gonçalves AC, Marques da Silva JR. Above Ground Biomass Estimation with High Spatial Resolution Satellite Images. *Biomass Volume Estimation and Valorization for Energy*. Rijeka: InTech; 2017. pp. 47-70
- [12] Fehrmann L, Kleinn C. General considerations about the use of allometric equations for biomass estimation on the example of Norway spruce in Central Europe. *Forest Ecology and Management*. 2006;**236**: 412-421
- [13] Eisfelder C, Kuenzer C, Dech S. Derivation of biomass information for semi-arid areas using remote-sensing data. *International Journal of Remote Sensing*. 2012;**33**:2937-2984
- [14] Gil A, Fonseca C, Benedicto-Royuela J. Land cover trade-offs in small Oceanic Islands: A temporal analysis of Pico Island, Azores. *Land Degradation & Development*. 2018;**29**:349-360
- [15] Baccini A, Laporte N, Goetz SJ, et al. A first map of tropical Africa's above-ground biomass derived from satellite imagery. *Environmental Research Letters*. 2008;**3**:045011
- [16] ESA. Biomass. Report for Mission Selection. An Earth Explorer to Observe Forest Biomass. Noordwijk, The Netherlands: SP-1324/1. European Space Agency; 2012

- [17] Le Toan T, Quegan S, Davidson MWJ, et al. The BIOMASS mission: Mapping global forest biomass to better understand the terrestrial carbon cycle. *Remote Sensing of Environment*. 2011;**115**:2850-2860
- [18] Carreiras JM, Quegan S, Le Toan T, et al. Coverage of high biomass forests by the ESA BIOMASS mission under defense restrictions. *Remote Sensing of Environment*. 2017;**196**:154-162
- [19] Sani DA, Hashim M, Hossain MS. Recent advancement on estimation of blue carbon biomass using satellite-based approach. *International Journal of Remote Sensing*. 2019;**40**:7679-7715
- [20] Kumar L, Sinha P, Taylor S, et al. Review of the use of remote sensing for biomass estimation to support renewable energy generation. *Journal of Applied Remote Sensing*. 2015;**9**:097696
- [21] Cavender-Bares J, Gamon JA, Townsend PA. *Remote Sensing of Plant Biodiversity*. Switzerland: Springer; 2020
- [22] Blackard JA, Finco MV, Helmer EH, et al. Mapping US forest biomass using nationwide forest inventory data and moderate resolution information. *Remote Sensing of Environment*. 2008;**112**:1658-1677
- [23] García M, Riaño D, Chuvieco E, et al. Estimating biomass carbon stocks for a Mediterranean forest in Central Spain using LiDAR height and intensity data. *Remote Sensing of Environment*. 2010;**114**:816-830
- [24] Los Soriano-Luna MDÁ, Ángeles-Pérez G, Guevara M, et al. Determinants of above-ground biomass and its spatial variability in a temperate Forest managed for timber production. *Forests*. 2018;**9**:490
- [25] Macedo FL, Sousa AM, Gonçalves AC, et al. Above-ground biomass estimation for *Quercus rotundifolia* using vegetation indices derived from high spatial resolution satellite images. *European Journal of Remote Sensing*. 2018;**51**:932-944
- [26] Pandit S, Tsuyuki S, Dube T. Estimating above-ground biomass in sub-tropical buffer zone community forests, Nepal, using sentinel 2 data. *Remote Sensing*. 2018;**10**:601
- [27] Stelmaszczuk-Górska M, Urbazaev M, Schmullius C, et al. Estimation of above-ground biomass over boreal forests in Siberia using updated In situ, ALOS-2 PALSAR-2, and RADARSAT-2 data. *Remote Sensing*. 2018;**10**:1550
- [28] Lu D, Weng Q. Spectral mixture analysis of the urban landscape in Indianapolis with Landsat ETM+ imagery. *Photogrammetric Engineering & Remote Sensing*. 2004;**70**:1053-1062
- [29] Nichol JE, Sarker MLR. Improved biomass estimation using the texture parameters of two high-resolution optical sensors. *IEEE Transactions on Geoscience and Remote Sensing*. 2011;**49**:930-948
- [30] Chen L, Wang Y, Ren C, et al. Optimal combination of predictors and algorithms for forest above-ground biomass mapping from sentinel and SRTM data. *Remote Sensing*. 2019;**11**:414
- [31] Gómez C, Wulder MA, Montes F, et al. Modeling forest structural parameters in the Mediterranean pines of Central Spain using QuickBird-2 imagery and classification and regression tree analysis (CART). *Remote Sensing*. 2012;**4**:135-159
- [32] Marshall M, Thenkabail P. Advantage of hyperspectral EO-1 Hyperion over multispectral IKONOS, GeoEye-1, WorldView-2, Landsat ETM+, and MODIS vegetation indices in crop

biomass estimation. *ISPRS Journal of Photogrammetry and Remote Sensing*. 2015;**108**:205-218

[33] Avitabile V, Baccini A, Friedl MA, et al. Capabilities and limitations of Landsat and land cover data for aboveground woody biomass estimation of Uganda. *Remote Sensing of Environment*. 2012;**117**:366-380

[34] Sinha S, Jeganathan C, Sharma LK, et al. A review of radar remote sensing for biomass estimation. *International journal of Environmental Science and Technology*. 2015;**12**:1779-1792

[35] Kasischke ES, Melack JM, Dobson MC. The use of imaging radars for ecological applications—A review. *Remote Sensing of Environment*. 1997; **59**:141-156

[36] Sandberg G, Ulander LM, Fransson JE, et al. L-and P-band backscatter intensity for biomass retrieval in hemiboreal forest. *Remote Sensing of Environment*. 2011;**115**:2874-2886

[37] Balzter H, Rowland CS, Saich P. Forest canopy height and carbon estimation at Monks Wood National Nature Reserve, UK, using dual-wavelength SAR interferometry. *Remote Sensing of Environment*. 2007;**108**:224-239

[38] Le Toan T, Beaudoin A, Riom J, et al. Relating forest biomass to SAR data. *IEEE Transactions on Geoscience and Remote Sensing*. 1992;**30**:403-411

[39] Carreiras JMB, Vasconcelos MJ, Lucas RM. Understanding the relationship between aboveground biomass and ALOS PALSAR data in the forests of Guinea-Bissau (West Africa). *Remote Sensing of Environment*. 2012; **121**:426-442

[40] Zebker HA, Van Zyl JJ, Held DN. Imaging radar polarimetry from wave synthesis. *Journal of Geophysical Research - Solid Earth*. 1987;**92**:683-701

[41] Carreiras J, Melo JB, Vasconcelos MJ. Estimating the above-ground biomass in miombo savanna woodlands (Mozambique, East Africa) using L-band synthetic aperture radar data. *Remote Sensing*. 2013;**5**: 1524-1548

[42] Liu Y, Gong W, Xing Y, et al. Estimation of the forest stand mean height and aboveground biomass in Northeast China using SAR sentinel-1B, multispectral sentinel-2A, and DEM imagery. *ISPRS Journal of Photogrammetry and Remote Sensing*. 2019;**151**:277-289

[43] Englhart S, Franke J, Keuck V, et al. Aboveground biomass estimation of tropical peat swamp forests using SAR and optical data. In: 2012 IEEE International Geoscience and Remote Sensing Symposium. IEEE; 2012. pp. 6577-6580

[44] Forkuor G, Zoungrana J-BB, Dimobe K, et al. Above-ground biomass mapping in West African dryland forest using Sentinel-1 and 2 datasets-A case study. *Remote Sensing of Environment*. 2020;**236**:111496

[45] Ghasemi N, Sahebi MR, Mohammadzadeh A. Biomass estimation of a temperate deciduous forest using wavelet analysis. *IEEE Transactions on Geoscience and Remote Sensing*. 2012;**51**:765-776

[46] Hayashi M, Motohka T, Sawada Y. Aboveground biomass mapping using ALOS-2/PALSAR-2 time-series images for Borneo's Forest. *IEEE Journal of Selected Topics in Applied Earth Observations and Remote Sensing*. 2019;**12**(12):5167-5177

[47] Morin D, Planells M, Guyon D, et al. Estimation and mapping of Forest structure parameters from open access satellite images: Development of a generic method with a study case on coniferous plantation. *Remote Sensing*. 2019;**11**:1275

- [48] Peregon A, Yamagata Y. The use of ALOS/PALSAR backscatter to estimate above-ground forest biomass: A case study in Western Siberia. *Remote Sensing of Environment*. 2013;**137**:139-146
- [49] Chen Q, Qi C. Lidar remote sensing of vegetation biomass. *Remote Sensing of Natural Resources*. 2013;**399**:399-420
- [50] Lucas R, Armston J, Fairfax R, et al. An evaluation of the ALOS PALSAR L-band backscatter—Above ground biomass relationship Queensland, Australia: Impacts of surface moisture condition and vegetation structure. *IEEE Journal of Selected Topics in Applied Earth Observations and Remote Sensing*. 2010;**3**:576-593
- [51] Englhart S, Keuck V, Siegert F. Aboveground biomass retrieval in tropical forests—The potential of combined X-and L-band SAR data use. *Remote Sensing of Environment*. 2011;**115**:1260-1271
- [52] Lu D. The potential and challenge of remote sensing-based biomass estimation. *International Journal of Remote Sensing*. 2006;**27**:1297-1328
- [53] Li G, Lu D, Moran E, et al. A comparative analysis of ALOS PALSAR L-band and RADARSAT-2 C-band data for land-cover classification in a tropical moist region. *ISPRS Journal of Photogrammetry and Remote Sensing*. 2012;**70**:26-38
- [54] Côté J-F, Fournier RA, Egli R. An architectural model of trees to estimate forest structural attributes using terrestrial LiDAR. *Environmental Modelling & Software*. 2011;**26**:761-777
- [55] Means JE, Acker SA, Harding DJ, et al. Use of large-footprint scanning airborne lidar to estimate forest stand characteristics in the Western cascades of Oregon. *Remote Sensing of Environment*. 1999;**67**:298-308
- [56] Maltamo M, Næsset E, Vauhkonen J. Forestry applications of airborne laser scanning. *Concepts, Methodologies and Case Studies*. 2014; **27**:460
- [57] Popescu SC, Wynne RH, Nelson RF. Measuring individual tree crown diameter with lidar and assessing its influence on estimating forest volume and biomass. *Canadian Journal of Remote Sensing*. 2003;**29**:564-577
- [58] Urbazaev M, Thiel C, Cremer F, et al. Estimation of forest aboveground biomass and uncertainties by integration of field measurements, airborne LiDAR, and SAR and optical satellite data in Mexico. *Carbon Balance and Management*. 2018;**13**:5
- [59] Ghosh SM, Behera MD. Aboveground biomass estimation using multi-sensor data synergy and machine learning algorithms in a dense tropical forest. *Applied Geography*. 2018;**96**: 29-40
- [60] Kattenborn T, Maack J, Nacht F, et al. Mapping forest biomass from space—fusion of hyperspectral EO1-hyperion data and Tandem-X and WorldView-2 canopy height models. *International Journal of Applied Earth Observation and Geoinformation*. 2015; **35**:359-367
- [61] Kellndorfer JM, Walker WS, LaPoint E, et al. Statistical fusion of Lidar, InSAR, and optical remote sensing data for forest stand height characterization: A regional-scale method based on LVIS, SRTM, Landsat ETM+, and ancillary data sets. *Journal of Geophysical Research – Biogeosciences*. 2010;**115**(G00E08)
- [62] Sun G, Ranson KJ, Guo Z, et al. Forest biomass mapping from lidar and radar synergies. *Remote Sensing of Environment*. 2011;**115**:2906-2916
- [63] Zheng D, Rademacher J, Chen J, et al. Estimating aboveground biomass

using Landsat 7 ETM+ data across a managed landscape in northern Wisconsin, USA. *Remote Sensing of Environment*. 2004;**93**:402-411

[64] Lu D, Batistella M. Exploring TM image texture and its relationships with biomass estimation in Rondônia, Brazilian Amazon. *Acta Amazonica*. 2005;**35**:249-257

[65] Mitchard ET, Saatchi SS, Lewis SL, et al. Measuring biomass changes due to woody encroachment and deforestation/degradation in a forest-savanna boundary region of Central Africa using multi-temporal L-band radar backscatter. *Remote Sensing of Environment*. 2011;**115**:2861-2873

[66] Saatchi S, Marlier M, Chazdon RL, et al. Impact of spatial variability of tropical forest structure on radar estimation of aboveground biomass. *Remote Sensing of Environment*. 2011;**115**:2836-2849

[67] Sarker MLR, Nichol J, Ahmad B, et al. Potential of texture measurements of two-date dual polarization PALSAR data for the improvement of forest biomass estimation. *ISPRS Journal of Photogrammetry and Remote Sensing*. 2012;**69**:146-166

[68] Popescu SC, Zhao K, Neuenschwander A, et al. Satellite lidar vs. small footprint airborne lidar: Comparing the accuracy of aboveground biomass estimates and forest structure metrics at footprint level. *Remote Sensing of Environment*. 2011;**115**:2786-2797

[69] Chao Z, Liu N, Zhang P, et al. Estimation methods developing with remote sensing information for energy crop biomass: A comparative review. *Biomass and Bioenergy*. 2019;**122**:414-425

[70] Lillesand T, Kiefer RW, Chipman J. *Remote Sensing and Image Interpretation*. New York: John Wiley & Sons; 2014

[71] Deng JS, Wang K, Deng YH, et al. PCA-based land-use change detection and analysis using multitemporal and multisensor satellite data. *International Journal of Remote Sensing*. 2008;**29**: 4823-4838

[72] Boardman JW, Kruse FA. Automated spectral analysis: A geological example using AVIRIS data, north Grapevine Mountains, Nevada. In: *Proceedings, ERIM Tenth Thematic Conference on Geologic Remote Sensing*. Ann Arbor, MI: Environmental Research Institute of Michigan; 1994. pp. I-407-I-418

[73] Green AA, Berman M, Switzer P, et al. A transformation for ordering multispectral data in terms of image quality with implications for noise removal. *IEEE Transactions on Geoscience and Remote Sensing*. 1988; **26**:65-74

[74] De Jong SM, Pebesma EJ, Lacaze B. Above-ground biomass assessment of Mediterranean forests using airborne imaging spectrometry: The DAIS Payne experiment. *International Journal of Remote Sensing*. 2003;**24**:1505-1520

[75] Kauth RJ, Thomas GS. The tasselled cap—a graphic description of the spectral-temporal development of agricultural crops as seen by Landsat. In: *LARS symposia*. 1976. p. 159

[76] Baig MHA, Zhang L, Shuai T, et al. Derivation of a tasselled cap transformation based on Landsat 8 at-satellite reflectance. *Remote Sensing Letters*. 2014;**5**:423-431

[77] Zhang X, Schaaf CB, Friedl MA, et al. MODIS tasseled cap transformation and its utility. In: *IEEE International Geoscience and Remote Sensing Symposium*. IEEE; 2002. pp. 1063-1065

[78] Crist EP, Kauth RJ. The Tasseled Cap de-mystified. *Photogrammetric*

Engineering and Remote Sensing. 1986; 52(1):81-86

[79] Ustin SL, Roberts DA, Gamon JA, et al. Using imaging spectroscopy to study ecosystem processes and properties. *Bioscience*. 2004;54:523-534

[80] Myneni RB, Hall FG, Sellers PJ, et al. The interpretation of spectral vegetation indexes. *IEEE Transactions on Geoscience and Remote Sensing*. 1995;33:481-486

[81] Jordan CF. Derivation of leaf-area index from quality of light on the forest floor. *Ecology*. 1969;50:663-666

[82] Carreiras JM, Pereira JM, Pereira JS. Estimation of tree canopy cover in evergreen oak woodlands using remote sensing. *Forest Ecology and Management*. 2006;223:45-53

[83] Gao B-C. NDWI—A normalized difference water index for remote sensing of vegetation liquid water from space. *Remote Sensing of Environment*. 1996;58:257-266

[84] Rouse JW, Haas RH, Schell JA, et al. Monitoring Vegetation Systems in the Great Plains with ERTS. In: *Third ERTS Symposium*, NASA SP-351. Washington DC. 1974. pp. 309-317

[85] Huete A, Didan K, Miura T, et al. Overview of the radiometric and biophysical performance of the MODIS vegetation indices. *Remote Sensing of Environment*. 2002;83:195-213

[86] Chen JM. Evaluation of vegetation indices and a modified simple ratio for boreal applications. *Canadian Journal of Remote Sensing*. 1996;22:229-242

[87] Lymburner L, Beggs PJ, Jacobson CR. Estimation of canopy-average surface-specific leaf area using Landsat TM data. *Photogrammetric Engineering and Remote Sensing*. 2000;66:183-192

[88] Huete A, Huete AR. A soil-adjusted vegetation index (SAVI). *Remote Sensing of Environment*. 1988;25: 295-309

[89] Deering DW. Measuring “forage production” of grazing units from Landsat MSS data. In: *Proceedings of the Tenth International Symposium of Remote Sensing of the Environment*. 1975. pp. 1169-1198

[90] Perry CR Jr, Lautenschlager LF. Functional equivalence of spectral vegetation indices. *Remote Sensing of Environment*. 1984;14:169-182

[91] Thiam AK. Geographic Information Systems and Remote Sensing Methods for Assessing and Monitoring Land Degradation in the Sahel Region: The Case of Southern Mauritania. Ph.D. dissertation. Worcester, Mass: Clark University; 1998

[92] Richardson AJ, Wiegand CL. Distinguishing vegetation from soil background information. *Photogrammetric Engineering and Remote Sensing*. 1977;43:1541-1552

[93] Baret F, Guyot G. Potentials and limits of vegetation indices for LAI and APAR assessment. *Remote Sensing of Environment*. 1991;35:161-173

[94] Crippen RE. Calculating the vegetation index faster. *Remote Sensing of Environment*. 1990;34:71-73

[95] Rondeaux G, Steven M, Baret F. Optimization of soil-adjusted vegetation indices. *Remote Sensing of Environment*. 1996;55:95-107

[96] Delegido J, Verrelst J, Alonso L, et al. Evaluation of sentinel-2 red-edge bands for empirical estimation of green LAI and chlorophyll content. *Sensors*. 2011;11:7063-7081

[97] Frampton WJ, Dash J, Watmough G, et al. Evaluating the

capabilities of Sentinel-2 for quantitative estimation of biophysical variables in vegetation. *ISPRS Journal of Photogrammetry and Remote Sensing*. 2013;**82**:83-92

[98] Zhou X, Dandan L, Huiming Y, et al. Use of landsat TM satellite surveillance data to measure the impact of the 1998 flood on snail intermediate host dispersal in the lower Yangtze River basin. *Acta Tropica*. 2002;**82**:199-205

[99] Gitelson AA, Kaufman YJ, Merzlyak MN. Use of a green channel in remote sensing of global vegetation from EOS-MODIS. *Remote Sensing of Environment*. 1996;**58**:289-298

[100] Birth GS, McVey GR. Measuring the color of growing turf with a reflectance spectrophotometer 1. *Agronomy Journal*. 1968;**60**:640-643

[101] Falkowski MJ, Gessler PE, Morgan P, et al. Characterizing and mapping forest fire fuels using ASTER imagery and gradient modeling. *Forest Ecology and Management*. 2005;**217**: 129-146

[102] Motohka T, Nasahara KN, Oguma H, et al. Applicability of green-red vegetation index for remote sensing of vegetation phenology. *Remote Sensing*. 2010;**2**:2369-2387

[103] Hardisky MA, Klemas V, Smart M. The influence of soil salinity, growth form, and leaf moisture on the spectral radiance of *Spartina alterniflora* canopies. *Photogrammetric Engineering and Remote Sensing*. 1983;**49**(1):77-83

[104] Hunt ER Jr, Rock BN. Detection of changes in leaf water content using near-and middle-infrared reflectances. *Remote Sensing of Environment*. 1989;**30**:43-54

[105] Haralick RM, Shanmugam KS, Dinstein I. Textural features for image classification. *IEEE Transactions on*

Systems, Man, and Cybernetics. 1973;**3**: 610-621

[106] Lu D. Aboveground biomass estimation using Landsat TM data in the Brazilian Amazon. *International Journal of Remote Sensing*. 2005;**26**:2509-2525

[107] Dube T, Mutanga O. Evaluating the utility of the medium-spatial resolution Landsat 8 multispectral sensor in quantifying aboveground biomass in uMgeni catchment, South Africa. *ISPRS Journal of Photogrammetry and Remote Sensing*. 2015;**101**:36-46

[108] Kayitakire F, Hamel C, Defourny P. Retrieving forest structure variables based on image texture analysis and IKONOS-2 imagery. *Remote Sensing of Environment*. 2006;**102**:390-401

[109] Chen D, Stow DA, Gong P. Examining the effect of spatial resolution and texture window size on classification accuracy: An urban environment case. *International Journal of Remote Sensing*. 2004;**25**:2177-2192

[110] Nyoungui AN, Tonye E, Akono A. Evaluation of speckle filtering and texture analysis methods for land cover classification from SAR images. *International Journal of Remote Sensing*. 2002;**23**:1895-1925

[111] Baccini A, Goetz SJ, Walker WS, et al. Estimated carbon dioxide emissions from tropical deforestation improved by carbon-density maps. *Nature Climate Change*. 2012;**2**:182

[112] Saatchi SS, Harris NL, Brown S, et al. Benchmark map of forest carbon stocks in tropical regions across three continents. *Proceedings of the National Academy of Sciences*. 2011;**108**:9899-9904

[113] Fassnacht FE, Hartig F, Latifi H, et al. Importance of sample size, data type and prediction method for remote sensing-based estimations of

aboveground forest biomass. *Remote Sensing of Environment*. 2014;**154**: 102-114

[114] Lu D, Chen Q, Wang G, et al. Aboveground forest biomass estimation with Landsat and LiDAR data and uncertainty analysis of the estimates. *International Journal of Forestry Research*. 2012;**2012**:1-16

[115] Liu K, Wang J, Zeng W, et al. Comparison and evaluation of three methods for estimating forest above ground biomass using TM and GLAS data. *Remote Sensing*. 2017;**9**:341

[116] Breiman L. Random forests. *Machine Learning*. 2001;**45**:5-32

[117] Guisan A, Edwards TC Jr, Hastie T. Generalized linear and generalized additive models in studies of species distributions: Setting the scene. *Ecological Modelling*. 2002;**157**:89-100

[118] Vapnik VN. *The Nature of Statistical Learning Theory*. Berlin: Springer Science & Business Media; 1999

[119] Foody GM, Cutler ME, McMorrow J, et al. Mapping the biomass of Bornean tropical rain forest from remotely sensed data. *Global Ecology and Biogeography*. 2001;**10**:379-387

[120] Willis MJ, Di Massimo C, Montague GA, et al. Artificial neural networks in process engineering. In: *IEE Proceedings D (Control Theory and Applications)*. IET; 1991. pp. 256-266

[121] Chen W, Chen J, Liu J, et al. Approaches for reducing uncertainties in regional forest carbon balance. *Global Biogeochemical Cycles*. 2000;**14**: 827-838

[122] Willmott CJ, Matsuura K. Advantages of the mean absolute error (MAE) over the root mean square error (RMSE) in assessing average model

performance. *Climate Research*. 2005; **30**:79-82

[123] Deo RK, Russell MB, Domke GM, et al. Using Landsat time-series and LiDAR to inform aboveground forest biomass baselines in northern Minnesota, USA. *Canadian Journal of Remote Sensing*. 2017;**43**:28-47

[124] Kennedy RE, Ohmann J, Gregory M, et al. An empirical, integrated forest biomass monitoring system. *Environmental Research Letters*. 2018;**13**:025004

[125] Matasci G, Hermosilla T, Wulder MA, et al. Three decades of forest structural dynamics over Canada's forested ecosystems using Landsat time-series and lidar plots. *Remote Sensing of Environment*. 2018;**216**:697-714

[126] Navarro JA, Algeet N, Fernández-Landa A, et al. Integration of uav, sentinel-1, and sentinel-2 data for mangrove plantation aboveground biomass monitoring in Senegal. *Remote Sensing*. 2019;**11**:77

[127] Townsend PA. Estimating forest structure in wetlands using multitemporal SAR. *Remote Sensing of Environment*. 2002;**79**:288-304

[128] Zhao P, Lu D, Wang G, et al. Forest aboveground biomass estimation in Zhejiang Province using the integration of Landsat TM and ALOS PALSAR data. *International Journal of Applied Earth Observation and Geoinformation*. 2016; **53**:1-15

[129] Naidoo L, Mathieu R, Main R, et al. L-band synthetic aperture radar imagery performs better than optical datasets at retrieving woody fractional cover in deciduous, dry savannahs. *International Journal of Applied Earth Observation and Geoinformation*. 2016;**52**:54-64

[130] Zeidler J, Wegmann M, Dech S. Spatio-temporal robustness of fractional

cover upscaling: A case study in semi-arid Savannah's of Namibia and Western Zambia. In: *Earth Resources and Environmental Remote Sensing/GIS Applications III*. International Society for Optics and Photonics; 2012. p. 85380S

[131] Ali I, Greifeneder F, Stamenkovic J, et al. Review of machine learning approaches for biomass and soil moisture retrievals from remote sensing data. *Remote Sensing*. 2015;7:16398-16421

[132] Ou G, Li C, Lv Y, et al. Improving aboveground biomass estimation of *Pinus densata* forests in Yunnan using Landsat 8 imagery by incorporating age dummy variable and method comparison. *Remote Sensing*. 2019;11:738

[133] Pflugmacher D, Cohen WB, Kennedy RE, et al. Using Landsat-derived disturbance and recovery history and lidar to map forest biomass dynamics. *Remote Sensing of Environment*. 2014;151:124-137

[134] Liu Y, Liu S, Li J, et al. Estimating biomass of winter oilseed rape using vegetation indices and texture metrics derived from UAV multispectral images. *Computers and Electronics in Agriculture*. 2019;166:105026

[135] Freeman EA, Moisen GG, Coulston JW, et al. Random forests and stochastic gradient boosting for predicting tree canopy cover: Comparing tuning processes and model performance. *Canadian Journal of Forest Research*. 2016;46:323-339

[136] Nguyen TH, Jones SD, Soto-Berelov M, et al. Monitoring aboveground forest biomass dynamics over three decades using Landsat time-series and single-date inventory data. *International Journal of Applied Earth Observation and Geoinformation*. 2020;84:101952

[137] Belgiu M, Drăguț L. Random forest in remote sensing: A review of applications and future directions. *ISPRS Journal of Photogrammetry and Remote Sensing*. 2016;114:24-31

[138] Li B, Wang W, Bai L, et al. Estimation of aboveground vegetation biomass based on Landsat-8 OLI satellite images in the Guanzhong Basin, China. *International Journal of Remote Sensing*. 2019;40:3927-3947

[139] Zhu X, Liu D. Improving forest aboveground biomass estimation using seasonal Landsat NDVI time-series. *ISPRS Journal of Photogrammetry and Remote Sensing*. 2015;102:222-231

[140] Sousa AM, Gonçalves AC, Mesquita P, et al. Biomass estimation with high resolution satellite images: A case study of *Quercus rotundifolia*. *ISPRS Journal of Photogrammetry and Remote Sensing*. 2015;101:69-79

[141] Debastiani AB, Sanquetta CR, Dalla Corte AP, et al. Evaluating SAR-optical sensor fusion for aboveground biomass estimation in a Brazilian tropical forest. *Annals of Forest Research*. 2019;62:109-122

[142] Laurin GV, Balling J, Corona P, et al. Above-ground biomass prediction by Sentinel-1 multitemporal data in Central Italy with integration of ALOS2 and Sentinel-2 data. *Journal of Applied Remote Sensing*. 2018;12:016008

[143] Godinho S, Guiomar N, Gil A. Estimating tree canopy cover percentage in a mediterranean silvopastoral systems using sentinel-2A imagery and the stochastic gradient boosting algorithm. *International Journal of Remote Sensing*. 2018;39:4640-4662

[144] Eckert S. Improved forest biomass and carbon estimations using texture measures from WorldView-2 satellite data. *Remote Sensing*. 2012;4:810-829

[145] Rao PN, Sai MS, Sreenivas K, et al. Textural analysis of IRS-1D panchromatic data for land cover classification. *International Journal of Remote Sensing*. 2002;**23**:3327-3345

[146] Fayad I, Baghdadi N, Bailly J-S, et al. Canopy height estimation in French Guiana with LiDAR ICESat/GLAS data using principal component analysis and random forest regressions. *Remote Sensing*. 2014;**6**:11883-11914

[147] Hlatshwayo ST, Mutanga O, Lottering RT, et al. Mapping forest aboveground biomass in the reforested Buffelsdraai landfill site using texture combinations computed from SPOT-6 pan-sharpened imagery. *International Journal of Applied Earth Observation and Geoinformation*. 2019;**74**:65-77

[148] Wulder M. Optical remote-sensing techniques for the assessment of forest inventory and biophysical parameters. *Progress in Physical Geography*. 1998; **22**:449-476

[149] Sarker LR, Nichol JE. Improved forest biomass estimates using ALOS AVNIR-2 texture indices. *Remote Sensing of Environment*. 2011;**115**: 968-977

[150] Patenaude G, Milne R, Dawson TP. Synthesis of remote sensing approaches for forest carbon estimation: Reporting to the Kyoto protocol. *Environmental Science & Policy*. 2005;**8**:161-178